JOURNAL OF VIROLOGY, Mar. 2009, p. 2188–2200 Vol. 83, No. 5
0022-538X/09/$08.00+0 doi:10.1128/JVI.02186-08

Diverse and Newly Recognized Effects Associated with Short Interfering RNA Binding Site Modifications on the *Tomato Bushy Stunt Virus* P19 Silencing Suppressor[▽]

Yi-Cheng Hsieh,[1] Rustem T. Omarov,[1] and Herman B. Scholthof[1,2]*

Department of Plant Pathology and Microbiology[1] and Intercollegiate Faculty of Virology,[2] Texas A&M University, 2132 TAMU, College Station, Texas 77843

Received 16 October 2008/Accepted 21 November 2008

The *Tomato bushy stunt virus*-encoded P19 forms dimers that bind duplex short interfering RNAs (siRNAs) to suppress RNA silencing. P19 is also involved in multiple host-specific activities, including the elicitation of symptoms, and in local and/or systemic spread. To study the correlation between those various roles and the siRNA binding by P19, predicted siRNA-interacting sites were modified. Twenty-two mutants were generated and inoculated onto *Nicotiana benthamiana* plants, to reveal that (i) they were all infectious, (ii) symptom differences did not correlate strictly with mutation-associated variation in P19 accumulation, and (iii) substitutions affecting a central domain of P19 generally exhibited symptoms more severe than for mutations affecting peripheral regions. Three mutants selected to represent separate phenotypic categories all displayed a substantially reduced ability to sequester siRNA. Consequently, these three mutants were compromised for systemic virus spread in P19-dependent hosts but had differential plant species-dependent effects on the symptom severity. One mutant in particular caused relatively exacerbated symptoms, exemplified by extensive morphological leaf deformations in *N. benthamiana*; this was especially remarkable because P19 was undetectable. Another striking feature of this mutant was that only within a few days after infection, viral RNA was cleared by silencing. One more original property was that host RNAs and proteins (notably, the P19-interactive Hin19 protein) were also susceptible to degradation in these infected *N. benthamiana* plants but not in spinach. In conclusion, even though siRNA binding by P19 is a key functional property, compromised siRNA sequestration can result in novel and diverse host-dependent properties.

RNA interference (RNAi), also known as RNA silencing or posttranscriptional gene silencing serves as a regulatory mechanism to target specific RNAs for degradation or translational repression and functions as a defense mechanism against viruses or invasive RNAs (2). RNA silencing is a conserved process in eukaryotes, including plants, single-celled algae, fungi, *Caenorhabditis elegans*, *Drosophila melanogaste*r, and mammalian cells (2, 3, 10, 17, 21, 60). The RNAi pathway is generally considered to be initiated with cleavage of a double-stranded RNA (dsRNA) by DICER-like complexes (3) into duplex short interfering RNAs (siRNAs) of ca. 20 to 25 nucleotides (nt) (11, 12). Subsequently, these ds-siRNAs are associated with the RNA induced silencing complex (RISC), where one of the strands remains bound and contributes to recognition of single-stranded RNAs (ssRNAs) targeted for cleavage (2, 3, 60).

To counter the silencing mechanism, viruses have evolved suppressors to combat the RNAi-mediated plant defense responses (4, 10, 16, 29, 32, 36, 37, 52). These suppressors, such as HC-Pro encoded by potyviruses (1, 14), 2b protein of cucumovirus (5), P19 of tombusviruses (28, 45, 55), P25 of potexviruses (56), the coat protein (CP) of carmoviruses (30, 48), and three RNAi suppressors encoded by *Citrus tristeza virus* (18), represent both nonstructural and structural proteins. Irrespective of this, most have in common that they were previously identified as pathogenicity factors or host range determinants (37). An example is the 19-kDa protein (P19) encoded by *Tomato bushy stunt virus* (TBSV) and related tombusviruses, perhaps representing one of the structurally best-studied and most widely used suppressors (38, 44, 47).

TBSV is the type member of the *Tombusvirus* genus (family *Tombusviridae*). It has a positive-sense ssRNA genome of ~4.8-kb encapsidated in isometric T=3 virus particles (23) and has a wide experimental host range (19, 33, 58). The TBSV RNA genome contains five open reading frames (ORFs): *p33* and *p92* (replication-associated), *p41* (coat protein), and the 3′-proximal nested genes *p22* and *p19* that encode a ~22-kDa protein (P22) and a ~19-kDa protein (P19), respectively (13, 33, 58). The *p19* ORF is entirely nested within that for *p22*; P19 has multiple roles in pathogenesis, and P22 is the cell-to-cell movement protein (MP) (58).

TBSV and related tombusviruses collectively provide a convenient model system to study RNAi (38, 44). Because virus replication is linked with the abundant accumulation of viral dsRNAs (40) and highly structured ssRNAs (20), these form suitable substrates for DICER-mediated cleavage to result in the accumulation of siRNAs, even though host RNA-dependent RNA polymerases (RdRPs) might also be involved in this process (53, 54). Regardless of their precise origin of biogenesis, siRNAs are produced, and these are readily sequestered by P19 to suppress RNA silencing to prohibit viral RNA degradation (15, 24, 25). P19 functions as a dimer (24, 27), and

* Corresponding author. Mailing address: Department of Plant Pathology and Microbiology, Texas A&M University, 2132 TAMU, College Station, TX 77843. Phone: (979) 862-1495. Fax: (979) 845-6483. E-mail: herscho@tamu.edu.

▽ Published ahead of print on 3 December 2008.

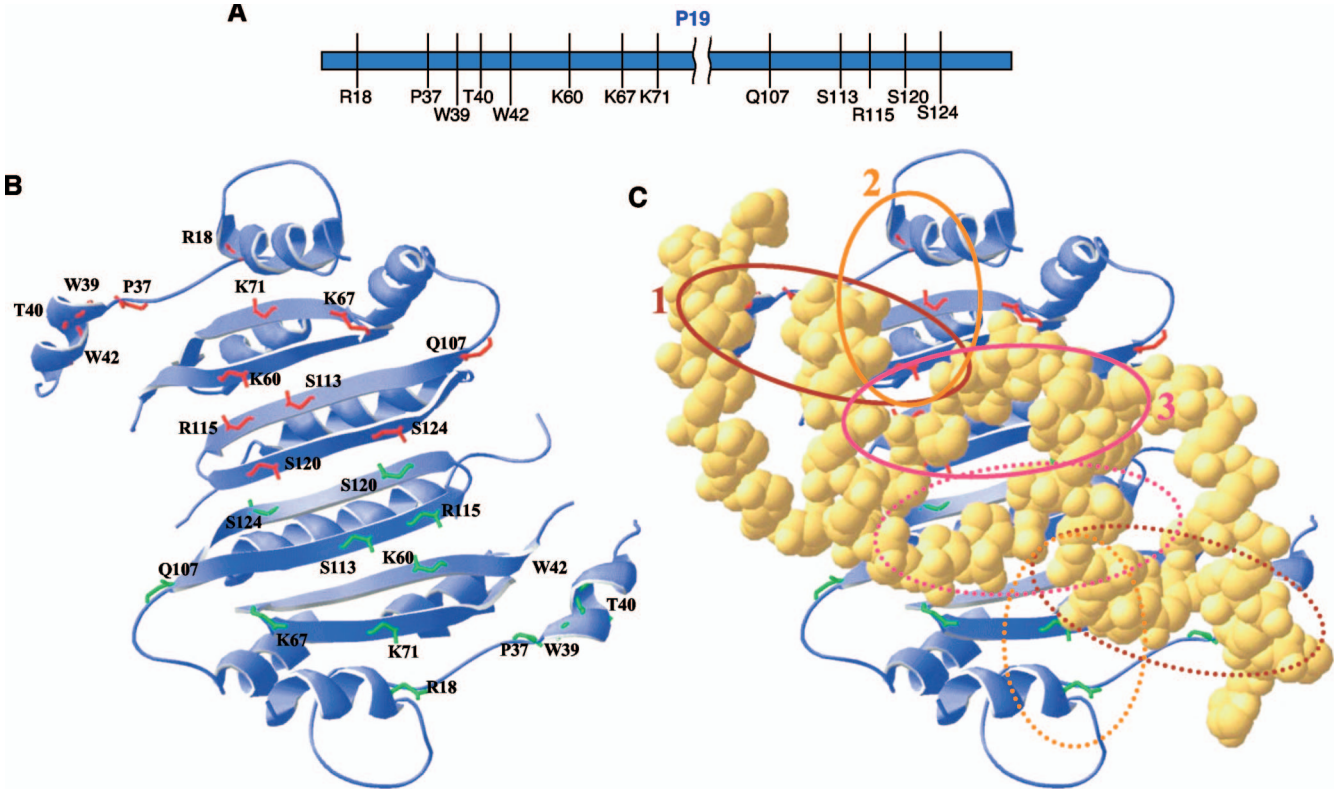

FIG. 1. Positions of siRNA binding sites on TBSV P19. (A) Diagram of selected P19 amino acids, which include P19/R18, P37, W39, T40, W42, K60, K67, K71, Q107, S113, R115, S120, and S124, to make single/combined amino acid substitutions. (B) Three-dimensional view of the siRNA binding sites shown as if viewed from the siRNA molecule (omitted here) projected down onto the protein dimer. The targeted amino acids on the two monomers of P19 are distinguished in red and green for each monomer, respectively. The parameters of the P19/siRNA structure were downloaded from the NCBI protein data bank (PDB) and analyzed by the Swiss PDB viewer. (C) The combination of amino acid substitutions was categorized into three main groups located on the external (group 1, brown circle), intermediate (group 2, orange circle), and central regions (group 3, red circle) of P19 dimers. The siRNA duplex is presented in yellow and the P19 dimer is displayed in blue. Solid circles indicate the three major domains on one of the monomers, and the dashed lines show the position on the other monomer.

X-ray crystallography of P19 showed that there are several positively charged amino acids available on the surface of P19 dimers to electrostatically interact size selectively with duplex siRNA molecules, most effectively with 21-nucleotide (nt) siRNAs (Fig. 1) (51, 59). Furthermore, the non-sequence-specific capture of siRNAs by P19 confers the ability of the protein to block RISC programming and to suppress the consequent hydrolysis of any RNA that is targeted by RNAi (15, 38, 44, 51, 55, 59).

Most studies on the activity of P19-mediated suppression have been performed in *Nicotiana* species, as well as *Arabidopsis* (not a host of TBSV) (7, 26, 55), but this does not accurately reflect the rather extensive host range (19, 58) and host-specific activities (38) of P19. For instance, activities of this protein include the elicitation of a hypersensitive response (HR) in *Nicotiana tabacum* (9, 41), promoting cell-to-cell movement in *Capsicum annuum* (pepper) (49), long-distance spread in pepper and *Spinacia oleracea* (spinach) (42, 49), and induction of severe symptom development in many plants (38).

P19 modifications that cause slight structural alterations were previously shown to compromise siRNA sequestration, which correlated with the recovery of plants from infection (24). However, these mutations did not specifically target siRNA-binding sites, and the structural effects also slightly compromised their binding to the interacting host factor Hin19 (27, 50). As such, it is not known whether the P19-siRNA binding sites predicted by the in vitro X-ray crystallography structure are important for any or all of the in vivo biological activities. This reflects the main question of the present study, and therefore we focused on investigating the diverse biological and biochemical effects of mutations designed to precisely perturb the interaction between P19 and siRNAs. For this purpose, we selected 13 sites on TBSV P19 that were predicted to contact siRNAs (51, 59) for mutagenesis, and these were examined either individually or cumulatively, for their effects on TBSV infection.

The results indicate that mutations affecting the periphery of the P19 dimer structure strongly attenuated symptoms on *N. benthamiana*, whereas those affecting a central region caused severe leaf deformations and stunting. Biochemical tests showed that siRNA binding was compromised for representative selected P19 mutants irrespective of the effect on symptoms. In addition, studies with plants other than *N. benthamiana* showed that symptom induction and systemic spread in some hosts correlated with the capacity of P19 to bind siRNAs, whereas this association was far less apparent for some biological features in other plant species. Intriguingly, one particular mutant caused the accelerated clearance of TBSV RNA and

protein degradation in infected *N. benthamiana* plants and, quite surprisingly, the levels of host RNA and proteins (especially the P19-interactive Hin19) were also substantially reduced in this host, whereas none of these effects were observed in spinach. In conclusion, substitutions on P19 that compromised siRNA binding not only impacted systemic invasion and symptom development but also resulted in newly recognized effects on the integrity of virus and host material in a plant species-dependent manner.

MATERIALS AND METHODS

Inoculation and analysis of plant tissues. Transcripts were generated in vitro from full-length TBSV cDNA plasmids expressing P19 derivatives. These plasmids (1 μg) were linearized at the 3′ terminus of the viral cDNA sequence by digestion with SmaI, and transcripts were synthesized by using T7 RNA polymerase. Plants were inoculated by using standard procedures (40). All infectivity studies and subsequent analyses were based on multiple repeats, and all plant species were grown under similar conditions to minimize the effect of environmental differences.

Site-directed mutagenesis. A QuikChange kit (Stratagene, La Jolla, CA) was used for site-directed mutagenesis, and standard molecular biology protocols (35) were followed for the isolation and manipulation of plasmid DNA. The plasmid used to generate mutants was a pUC119 phagemid derivative containing a full-length TBSV cDNA insert encoding one amino acid substitution of P19/K60A (9). All constructs were designed to cause substitutions on P19, while keeping the P22 protein specified by the overlapping ORF intact.

RNA analysis. Total RNA was extracted by grinding ~200 mg of leaf material (inoculated or systemically infected leaves) on ice in 1 ml of extraction buffer (100 mM Tris-HCl [pH 8.0], 1 mM EDTA, 0.1 M NaCl, 1% sodium dodecyl sulfate [SDS]). The homogenates were immediately extracted twice with phenol-chloroform (1:1 [vol/vol]), and total RNAs were precipitated with 8 M lithium chloride solution (1:1 [vol/vol]) at 4°C for 15 to 25 min. The resulting pellets were washed with 70% ethanol and then resuspended in RNase-free distilled water. Approximately 10 μg of total RNA was separated on a 1% agarose gel in 1× Tris-borate-EDTA buffer, followed by transfer to nylon membranes (Osmonics, Westborough, MA) for Northern hybridization analysis with [^{32}P]dCTP-labeled TBSV-specific probes, as previously described (40, 42).

Detection of TBSV-derived siRNAs. P19/siRNA complexes purified by immunoprecipitation were treated with 10% SDS at 65°C for 15 min, followed by phenol-chloroform extraction, and siRNAs were ethanol precipitated and further processed as in a prior report (24). Subsequently, siRNAs were separated by electrophoresis through a 17% polyacrylamide gel (with 8 M urea), after which the proteins were electrotransferred onto nylon membrane (Osmonics) and analyzed by hybridization with TBSV-specific dCTP-^{32}P-labeled probes at 42°C. In addition, total RNAs were also extracted from infected plants and analyzed essentially as described above, as detailed previously (24).

Western blot analysis. Protein samples were prepared as described previously (43) and then separated by SDS-polyacrylamide gel electrophoresis (PAGE) in 15% polyacrylamide gels, followed by transfer to nitrocellulose membranes (Osmonics). The membranes were stained with Ponceau S (Sigma, St. Louis, MO) to verify the efficiency of protein transfer. Antisera specific for detection of individual TBSV proteins were applied at the dilution of 1:5,000 (41). Alkaline phosphatase-conjugated goat anti-mouse or anti-rabbit antiserum (Sigma) was used as the secondary antibody and applied at a dilution of 1:1,000. The immune complexes were visualized by hydrolysis of tetrazolium-BCIP (5-bromo-4-chloro-3-indolylphosphate) as the substrate in the presence of nitroblue tetrazolium chloride.

Immunoprecipitation. Fresh leaf tissue (1 g) was swiftly pulverized in an ice-cold mortar with 1.5 ml of ice-cold extraction buffer (150 mM HEPES [pH 7.5], 200 mM NaCl, 1 mM EDTA, 2 mM dithiothreitol) containing protease inhibitor cocktail (Roche Diagnostics, Indianapolis, IN). The homogenate was filtered through cheesecloth and centrifuged twice at 10,000 × g at 4°C for 15 min. Then, 800 μl of the supernatant was incubated at a 1:400 dilution with TBSV-P19 rabbit polyclonal antibodies at 4°C for 2 h, after which 30 μl of ImmunoPure immobilized protein G agarose beads (Pierce, Rockford, IL) was added. The samples were incubated for an additional 2 h at room temperature, and then the beads were collected by brief centrifugation and washed with ice-cold extraction buffer; this was repeated six times. The precipitated proteins were analyzed by SDS-PAGE, followed by Western blotting.

RESULTS

Effect of P19-siRNA contact site modifications on symptom development in *N. benthamiana*. The mutations indicated in Fig. 1 and Table 1 were introduced on the previously mutated infectious TBSV construct expressing P19/K60A that affected one potential siRNA binding site. This mutation somewhat attenuated symptoms on *N. benthamiana* but had no noticeable effect on HR in *N. tabacum* or systemic invasion of spinach (9). Thus, in anticipation that cumulative mutations would further affect the functionality, we selected P19/K60A expressing cDNA as the parental construct to add additional mutations. We chose not to use the wild-type *p19* gene as the backbone for mutagenesis, since its expression is lethal to many plants, and thus any mutation that could exacerbate symptoms would become masked in the wild-type background.

Since the ORF for translation of the P22 cell-to-cell movement protein entirely overlaps with the *p19* ORF, this limited the available options for the type of nucleotide substitution that could be introduced without changing the *p22* sequence. Consequently, mutations were made to result in the single amino acid replacements R18C, P37S, W39G, T40S, W42R, K67E, K71E, Q107P, S113C, R115W, S120G, and S124P (Fig. 1 and Table 1), and certain mutations were combined for sites close to each other from a three-dimensional perspective (Fig. 1).

Based on symptoms, Western blots, Northern blots, or combinations thereof, it was evident that all *p19* mutants were able to initially establish full systemic infections on *N. benthamiana*. This is consistent with the currently commonly known property that the *Tombusvirus* P19 has no discernible effects in *N. benthamiana* regarding replication, cell-to-cell movement, and the initiation of a systemic infection (38). Furthermore, the nonlethal phenotypes associated with most mutants in this host were not reversed to lethal upon superinfection of plants with wild-type TBSV (wtTBSV; data not shown), indicating that introduction of wtP19 in these plants did not reverse the programming of the already established anti-TBSV RISC (24). This type of cross-protection is also in agreement with the conclusion that the plants were indeed systemically infected with the mutants.

Symptoms and relative P19 accumulation for all twenty-two mutants on *N. benthamiana* are summarized in Table 1, and Fig. 2 shows a representative for each of the main phenotypic categories. The lethal necrotic symptoms on *N. benthamiana* were only observed for plants infected with TBSV expressing wtP19, typically resulting in severe symptoms on the inoculated leaves starting at 3 days postinfection (dpi) and the upper leaves at 5 dpi, followed within a few days by apical necrosis and eventual systemic collapse (Fig. 2). TBSV expressing P19/K60A (parental construct for mutagenesis) showed attenuated symptoms upon infection and, as expected, many P19 derivatives with additional mutations caused even milder symptoms (Table 1 and Fig. 2). However, surprisingly, not all additional mutations had additive attenuation effects because some combinations of mutations caused more severe symptoms than those observed for P19/K60A (Table 1 and Fig. 2). There was no obvious correlation between the number of siRNA sites targeted for each mutant or the relative level of P19 accumulation, and the effect on symptoms. However, while comparing

TABLE 1. Severity of symptoms in *N. benthamiana* associated with P19 mutations

P19 mutation(s)[a]	Amino acid at position:													Severity and P19 content[b]		Group[c]
	18	37	39	40	42	60	67	71	107	113	115	120	124	Severity	P19 content	
P19 (wild type)	R	P	W	T	W	K	K	K	Q	S	R	S	S	+++++	+++++	
P19/60	R	P	W	T	W	A	K	K	Q	S	R	S	S	+++	+++++	*
P19/18-60	**C**	P	W	T	W	A	K	K	Q	S	R	S	S	+++	++++	2
P19/37-60	R	**S**	W	T	W	A	K	K	Q	S	R	S	S	++	++	1
P19/37-39-60	R	**S**	**G**	T	W	A	K	K	Q	S	R	S	S	+	+++	1
P19/42-60	R	P	W	T	**R**	A	K	K	Q	S	R	S	S	+++	+++	1
P19/37-39-40-42-60 (M1)	R	**S**	**G**	**S**	**R**	A	K	K	Q	S	R	S	S	+	+++	1
P19/60-67	R	P	W	T	W	A	**E**	K	Q	S	R	S	S	++	+++++	2, x
P19/60-71	R	P	W	T	W	A	K	**E**	Q	S	R	S	S	++	+++++	2
P19-18-60-71 (M2)	**C**	P	W	T	W	A	K	**E**	Q	S	R	S	S	+	+++++	2
P19/60-107	R	P	W	T	W	A	K	K	**P**	S	R	S	S	++	+	3, x
P19/60-67-107	R	P	W	T	W	A	**E**	K	**P**	S	R	S	S	+	++++	x
P19/60-113	R	P	W	T	W	A	K	K	Q	**C**	R	S	S	++++	++++	3
P19/60-107-113	R	P	W	T	W	A	K	K	**P**	**C**	R	S	S	++++	++++	3, x
P19/60-115	R	P	W	T	W	A	K	K	Q	S	**W**	S	S	++++	+++++	3
P19/60-107-113-115	R	P	W	T	W	A	K	K	**P**	**C**	**W**	S	S	+	++++	3, x
P19/60-120	R	P	W	T	W	A	K	K	Q	S	R	**G**	S	+	+++++	3
P19/60-113-120	R	P	W	T	W	A	K	K	Q	**C**	R	**G**	S	+	+++++	3
P19/60-115-120	R	P	W	T	W	A	K	K	Q	S	**W**	**G**	S	++	+++++	3
P19/60-124	R	P	W	T	W	A	K	K	Q	S	R	S	**P**	+++	+++	3
P19/60-120-124	R	P	W	T	W	A	K	K	Q	S	R	**G**	**P**	++	++	3
P19/60-115-120-124	R	P	W	T	W	A	K	K	Q	S	**W**	**G**	**P**	++++	–	3
P19/60-113-115-120-124 (M3)	R	P	W	T	W	A	K	K	Q	**C**	**W**	**G**	**P**	++++	–	3

[a] The numbers indicate residues on P19 that were substituted, and the subsequent columns give the amino acids at specific positions, with the boldface residues specifying substitutions compared to the parental construct P19/60 used for mutagenesis. The wild-type P19 with K60 is given in the top row for comparison to P19/60.

[b] The "+" symbols indicate the relative symptom severity and the relative P19 accumulation for infected *N. benthamiana* plants. The relative level of P19 reflects a classification that is an average based on several Western assays similar to that depicted in Fig. 3. See legend to Fig. 2 for scoring key for symptoms.

[c] The numbers denote the domain (see Fig. 1) that was affected; the asterisk (*) indicates that the residue at position 60 is located at the intersection of the three domains; "x" indicates that the two amino acids, K67 and Q107, are located just outside domain 2 or 3.

symptom severity (Table 1) with the structural distribution of mutations (Fig. 1), a trend surfaced that substitutions (in addition to K60A) positioned on the peripheral regions of the P19 dimer (domain 1) mostly resulted in attenuated symptoms. In contrast, changes affecting the central domain of P19 dimer (domain 3) caused mostly severe phenotypes (albeit less severe than for wtP19), with the exception of S120G. Substitutions positioned in between (domain 2) generally were associated with intermediate symptoms.

Extracts from infected *N. benthamiana* plants were subjected to Western blotting for the detection of P19, as shown for 13 of the 22 mutants in Fig. 3 and indicated for all mutants in Table 1. Notably, the accumulation of P19 monomers was reduced for some mutants in Fig. 3, for instance in lanes 4 and 8, even though the amount of (SDS-recalcitrant) P19 dimers for these samples was not substantially less than that observed for those in adjacent lanes. However, for mutants with the S124P substitution (lanes 10, 12, and 13 in Fig. 3 and see the bottom of Table 1), the amounts of P19 monomers or dimers were either barely detectable or not detectable. The differences in levels of P19 observed for mutants at 5 dpi (Fig. 3), which were already noticeable at 3 dpi (not shown), were a reflection of accumulation of total viral material as it was mirrored by similar differences in CP and P22 measured in parallel (results not shown). The reduced levels or absence of virus material forms

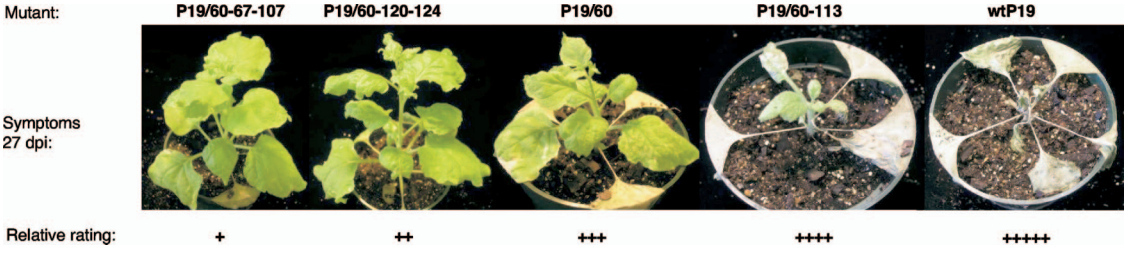

FIG. 2. Representative phenotypes of TBSV infections influenced by modifications on P19. The inoculated plants were categorized into different levels as also indicated in Table 1 to describe the severity of symptoms from of P19 derivatives on *N. benthamiana*. In order not to miss delayed onset of symptoms, plants were photographed at 27 dpi. For the categorization (also used in Table 1) the parental construct used for mutagenesis (P19/60) was classified as exhibiting intermediate (+++) symptoms, while wtTBSV expressing wtP19 displayed a lethal (+++++) phenotype; P19/60-67-107 and P19/60-120-124 induced very mild (+) or moderately aggressive (++) symptoms, whereas P19/60-113 caused nonlethal but clearly noticeable necrotic symptoms (++++).

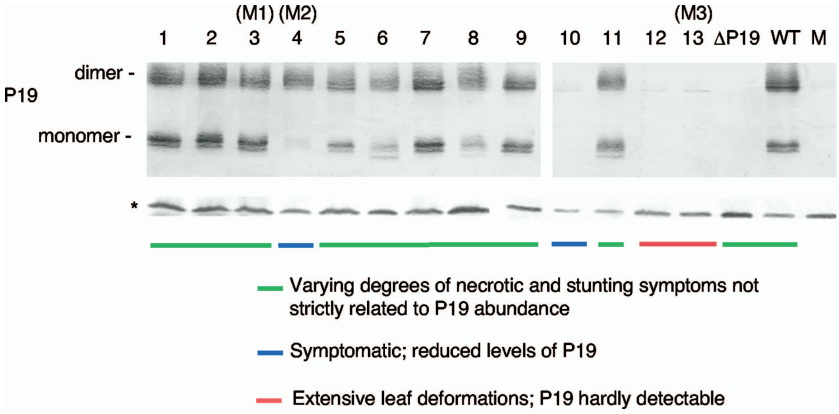

FIG. 3. Accumulation of mutant P19 proteins upon infection of *N. benthamiana*. Western blot detection of P19 proteins from plant tissues at 5 dpi: P19/60, lane 1; P19/37-39-60, lane 2; P19/37-39-40-42-60, lane 3; P19/18-60-71, lane 4; P19/60-67-107, lane 5; P19/60-107-113-115, lane 6; P19/60-120, lane 7; P19/60-113-120, lane 8; P19/60-115-120, lane 9; P19/60-120-124, lane 10; P19/60-113, lane 11; P19-60-115-120-124, lane 12; P19/60-113-115-120-124, lane 13. All mutants were compared to wild-type P19 (WT) and P19-defective (ΔP19) associated infections and with mock-inoculated (M) samples. The mutants referred to as M1, M2, and M3 later in the study are indicated. The color lines indicate the effect of the mutants on symptoms and P19 accumulation; a representative of each color (M1 to M3) was selected. Rabbit P19 antiserum was used for protein detection. The unspecific ~23-kDa host protein recognized by this P19 antiserum served as a loading control, indicated by an asterisk (*), that was present in the insoluble fraction but undetectable in the cytosolic fraction of the same samples containing P19 (upper panel).

an intriguing contrast to the serious systemic symptoms observed for many of these mutants (Table 1, Fig. 2, and Fig. 3).

Effect of P19 modifications on siRNA accumulation and sequestration. Based on the observed correlations between the domain position of mutations (Fig. 1, Fig. 2, and Table 1) and the effect on symptoms in infected *N. benthamiana*, in combination with the reduced level of P19 accumulation associated in some instances (Fig. 3), representatives of contrasting mutants were selected for a more detailed analysis (see Fig. 3). The selected mutants were (i) P19/37-39-40-42-60 (hereafter referred to as M1 for simplicity), affecting domain 1 that includes the reading head that "measures" the size of siRNAs, causing substantial symptom attenuation, and having minimal effect on P19 accumulation; (ii) P19/18-60-71 (M2) affecting domain 2, resulting in attenuated symptoms while reducing total levels of P19 accumulation; and (iii) P19/60-113-115-120-124 (M3), affecting domain 3 causing relatively severe leaf deforming symptoms, and P19 was reduced to virtually undetectable levels.

Prior to siRNA analyses, total proteins were collected from plants at 7 dpi, and the Western blot analyses for detection of P19 (Fig. 4A, top left panel) essentially verified what was observed at 5 dpi (Fig. 3), that no detectable levels of P19 protein were present for M3 (Fig. 4A). Immunoprecipitation of *N. benthamiana* extracts with P19-specific antiserum was then performed to pull down associated siRNAs for each selected P19 derivative. Western analysis of precipitated P19 (Fig. 4A, top right panel) displayed monomers and dimers, or the absence thereof, similar to what was observed for total extracts (Fig. 4, top left panel). The relevance of faint bands for some samples at other positions is not known (see the legend for Fig. 4A).

The detection of TBSV-siRNAs in total RNA extracts from infected plants revealed that infections with the M1, M2, and ΔP19 mutants yielded viral siRNAs at levels comparable to that observed for wtP19 (Fig. 4B, left panel). However, in plants infected with the M3 mutant, no siRNAs were detected at this time point (7 dpi; Fig. 4B, left panel), although at 3 dpi a weak signal could be observed (data not shown). Analysis of siRNAs in P19 immunoprecipitation samples showed that wtP19 was associated with TBSV-specific ~21-nt siRNAs, whereas this was not detectable for P19 of M1 to M3 (Fig. 4B, right panel). Thus, there was no consistent correlation between the compromised association of P19 with siRNAs in these tests and the effect on symptom severity in *N. benthamiana* (Table 1). However, it is evident that the mutations influenced siRNA sequestration and that this eventually resulted in a recoverylike phenotype in most cases at several weeks after inoculation, a finding similar to what is known for P19 defective or null mutants (24).

A serendipitous finding was that ethidium bromide (EtBr) staining of agarose gels demonstrated that total RNA extracted from symptomatic plants contained a readily visible fast-migrating band underneath the 5S rRNA that was not present in samples from healthy or mock-inoculated plants (Fig. 4C). Extraction of this virus-specific band, followed by denaturing gel electrophoresis and Northern hybridization, confirmed that the short RNAs were double stranded and derived from TBSV (data not shown). Based on repetitions, comparison of the EtBr intensities of this band in this very simple assay for the different samples correlated with differences in intensities observed in the much more laborious siRNA detection technique (Fig. 4B, left).

Host-specific effects of selected P19 mutants. If siRNA binding by P19 would be the sole biochemical property controlling its various biological activities in the different TBSV hosts, then it could be surmised that the M1, M2, and M3 mutants would display similar defective phenotypes in each plant species compared to infections with wild-type virus. To test this, we monitored symptom induction on inoculated leaves of *Cucurbita maxima* (pumpkin), *N. gossei*, *N. tabacum*, *Spinacia oleracea* (spinach), and *Vigna unguiculata* (cowpea). It is important to note that in *N. tabacum* P19 is known to be the elicitor of an HR (41), whereas this role of P19 has not yet

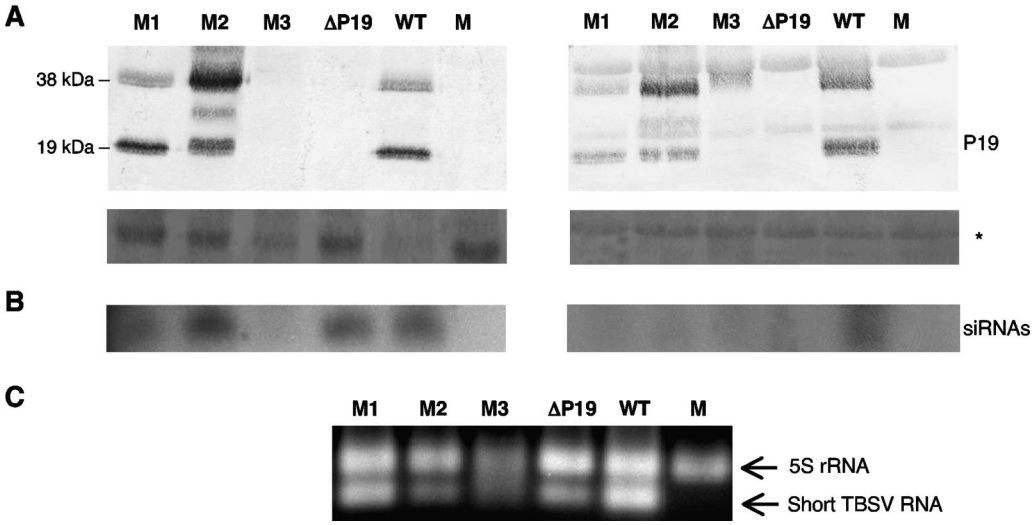

FIG. 4. P19 accumulation and siRNA binding of selected TBSV P19 mutants. (A) Western blot analysis of P19 from the total protein samples (left) and upon immunoprecipitation with P19 antiserum (right) from *N. benthamiana*. Total proteins and immunoprecipitation samples were obtained from *N. benthamiana* plants infected with TBSV expressing M1, M2, M3, ΔP19, and wtP19 (WT) at 7 dpi. Rabbit P19 antiserum was used for precipitating complexes; mouse P19 antiserum was utilized for detecting proteins from these P19 derivatives and mock treatment (M). The signals for immune complexes were determined by a colorimetric alkaline phosphatase reaction. Ponceau S staining after transfer from SDS-PAGE gels was used to compare sample loading (indicated by the asterisk). A nonspecific host protein that is reduced for the wild type, presumably due to the onset of a lethal collapse but also for M3 (to be discussed later), is shown on the left; in the right panel the band represents the antibody heavy chain. For M2, an additional P19 mouse-antibody cross-reacting polypeptide was reproducibly observed that migrated between the dimer and the monomer of P19 (left and right panel), but its relevance is unknown. Neither is the origin or significance known at this time of the additional band for M3/P19 that migrated above the P19 dimer on the right side panel. (B) Northern blot analysis of TBSV-derived small RNAs in total RNAs is shown in the left panel at 7 dpi; the right panel displays the detection of siRNAs coimmunoprecipitated with P19. (C) EtBr staining of agarose gels revealed the presence of a small RNA species (indicated by an arrow underneath the 5S rRNA) in the total RNAs that was observed at 7 dpi (left) and could be used as an indicator of TBSV infection.

been established for other plants. The effects of the mutations for systemic symptoms were compared for *N. benthamiana*, *N. excelsior*, and *C. annuum* (pepper) (Table 2). Symptoms induced for selected plants are shown in Fig. 5.

The first noticeable observation from examining Table 2 and Fig. 5 is that TBSV was only able to elicit local lesions on *N. gossei* or to induce systemic symptoms in pepper, when expressing wtP19, implying a probable correlation between the ability of P19 to sequester siRNAs and infection of these hosts. Another finding was that the mutants M1 and M2 behaved similarly in most hosts (except in *N. tabacum*) as typified by the induction of relatively mild symptoms. In comparison, M3 was generally associated with more severe symptomatic effects (Table 2 and Fig. 5).

Even though TBSV initiates a systemic infection on *N. benthamiana* in the absence of P19 (Fig. 5), it was previously shown that this protein is needed for systemic invasion of spinach (9, 42). Since the accumulation of P33 is known to correlate directly with virus replication and cell-to-cell movement in spinach (39), the mutants were examined for their ability to infect spinach, by monitoring the accumulation of viral proteins P33 and P19 (Fig. 6). The results showed that both proteins accumulated to detectable levels in inoculated spinach leaves (which is consistent with the induction of visible symptoms in Fig. 5). In upper leaves, no P33 was detected for any P19 mutants, whereas trace amounts of P19 were detected for mutants M1 and M3 (but not for M2 and ΔP19) (Fig. 6). This sustainable (Fig. 6, left panel) and systemic (Fig. 6, right panel) accumulation of P19 for M3 in spinach contrasts to what was observed for this mutant in *N. benthamiana*, where no or strongly reduced levels of viral protein accumulated (Fig. 3 and 4). That infections with the three siRNA-binding mutants (M1

TABLE 2. Host-specific pathogenic effects associated with P19 mutants[a]

Construct	Local symptoms					Systemic symptoms		
	Pumpkin	*N. gossei*	*N. tabacum*	Spinach	Cowpea	Pepper	*N. benthamiana*	*N. excelsior*
wtTBSV	+++	+++	+++	+++	+++	+++	+++	+++
ΔP19	?	–	–	–	+++	–	++	++
P19/37-39-40-42-60 (M1)	+	–	+	++	+	–	+	+
P19/18-60-71 (M2)	+	–	–	++	+	–	+	+
P19/60-113-115-120-124 (M3)	+++	–	++	+++	++	–	+++	+++
Mock	–	–	–	–	–	–	–	–

[a] Host-specific pathogenic effects were tested for TBSV expressing P19 mutants or wtP19. The plants tested included pumpkin (*C. maxima*), *N. gossei*, *N. tabacum*, spinach (*S. oleracea*), cowpea (*V. unguiculata*), pepper (*C. annuum*), *N. benthamiana*, and *N. excelsior*.

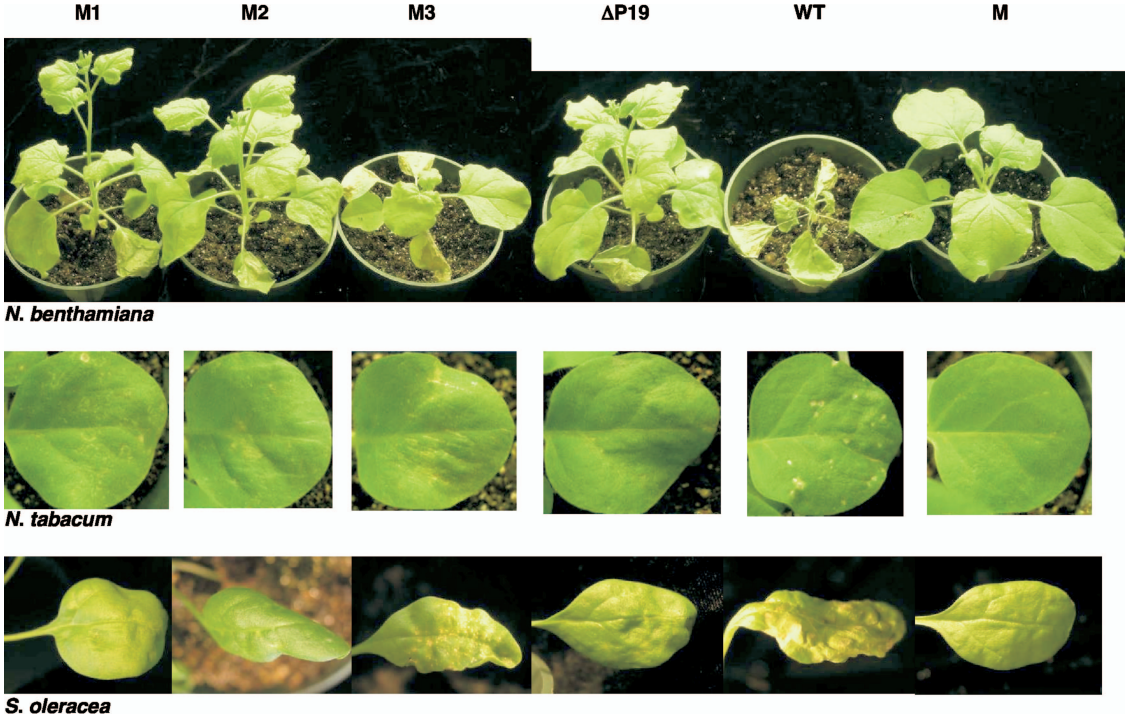

FIG. 5. Responses of different host plants upon infection with mutants M1, M2, and M3. Transcripts of mutants were inoculated onto *N. benthamiana*, *N. tabacum*, and *S. oleracea*, and the subsequent symptom generation was monitored. The P19 derivatives include M1, M2, M3, ΔP19, and wtP19 (WT); a mock treatment (M) was also included.

to M3) did not result in the accumulation of detectable amounts of P33 (Fig. 6) and CP (data not shown) in upper spinach leaves implies that siRNA binding by P19 is important for TBSV to establish a full systemic infection in this host.

Together, these results suggest that changes of siRNA binding sites that compromise the sequestration of siRNAs modulate invasive capacity and symptom induction in some hosts, whereas in other species the ability for siRNA binding is not strictly correlated with pathogenicity. This supports an interpretation favoring the existence of a host-differential impact of P19-siRNA binding site modifications.

Effects of M3 mutations on the integrity of virus and host RNAs and proteins. In order to understand the biochemical basis for the aberrant behavior of the M3 mutant, this derivative was subjected to closer scrutiny. First, to determine whether the remarkable symptomatology associated with M3 in *N. benthamiana* reflects a unique response, this mutant was also inoculated onto *N. excelsior*, which is distinct from *N. benthamiana* but similarly susceptible for systemic infection with TBSV. As is evident in Fig. 7, infection of *N. benthamiana* and *N. excelsior* plants with TBSV expressing wtP19 led to a lethal necrosis in both hosts. Even though infection with M3

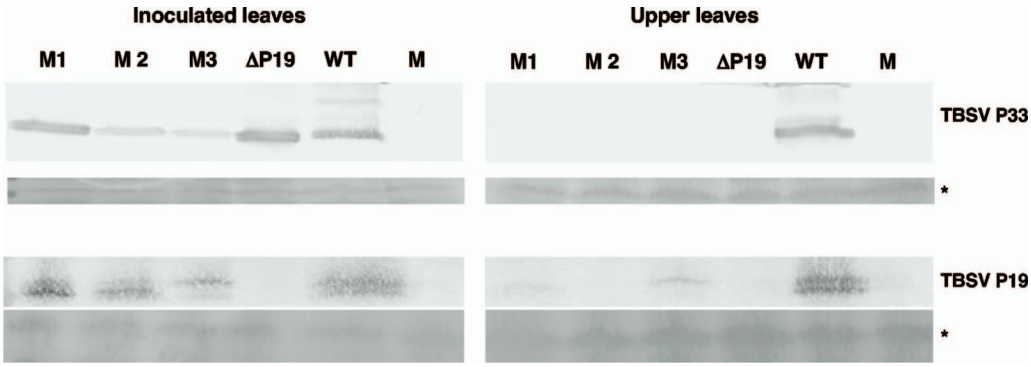

FIG. 6. Effects of P19 modifications on virus accumulation in spinach. The panels show the immunodetection of TBSV P33 or P19 as indicated, in inoculated (left) and upper (right) leaves of spinach (*S. oleracea*) at 12 dpi. The reason why P19 is sometimes detected as a duplet is not known at this point. The panels marked with an asterisk show an unidentified host protein that served as an internal loading control for SDS-PAGE upon Ponceau S staining. The abbreviations are as defined in previous figures.

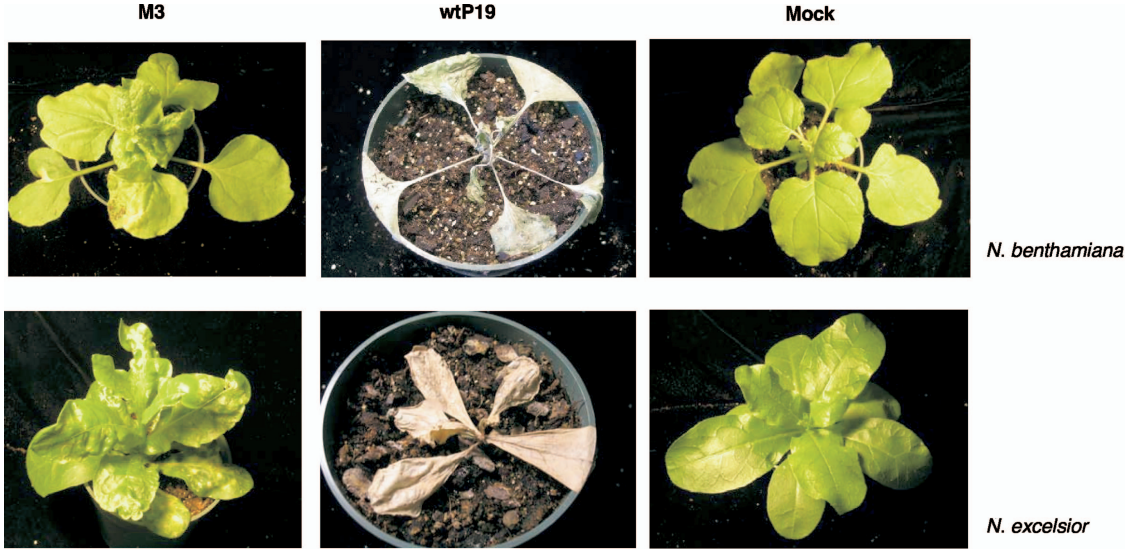

FIG. 7. Host-specific symptom development associated with M3. M3 and wtTBSV transcripts were inoculated onto *N. benthamiana* and *N. excelsior*, and the symptoms were monitored. TBSV expressing wtP19 resulted in the death of both hosts, while M3 generated saw-toothed, curling, bushy leaves with some lesions in *N. excelsior* (bottom left).

was not lethal, the symptoms, especially leaf deformations, were quite extensive and similar for both species (Fig. 7). Therefore, the symptoms associated with M3 are not an aberrance in *N. benthamiana* but might reflect a more general response in susceptible *Nicotiana* species. Intuitively, the severe systemic symptoms associated with M3 seem to conflict with the observation that TBSV proteins are undetectable in *N. benthamiana* infected with this mutant (Fig. 3 and 4 and data not shown), and this will be addressed more extensively below.

To determine the effects of mutations on viral RNA maintenance (i.e., RNA silencing), *N. benthamiana* samples were harvested at 3 and 5 dpi (Fig. 8), and at 7 dpi (Fig. 9A), and total RNAs were extracted and subjected to Northern blot hybridization. TBSV genomic RNA, subgenomic RNA1, and subgenomic RNA2 were detected at 3 dpi for plants infected with TBSV expressing M1, M2, M3, ΔP19, and wtP19 (Fig. 8). However, much-reduced levels of viral RNAs were present for M3 2 days later compared to the other samples, with gRNA being the most affected (Fig. 8 and Fig. 9A). For *N. benthamiana* plants infected with TBSV-ΔP19, clearing of viral RNAs generally takes 2 weeks (22). Thus, it seems that the M3 mutations have dramatically accelerated the impact of RNA silencing on viral maintenance. This once more contrasts with the serious symptoms (Fig. 5). Moreover, when examining the levels of total RNA (Fig. 9), it was reproducibly observed that

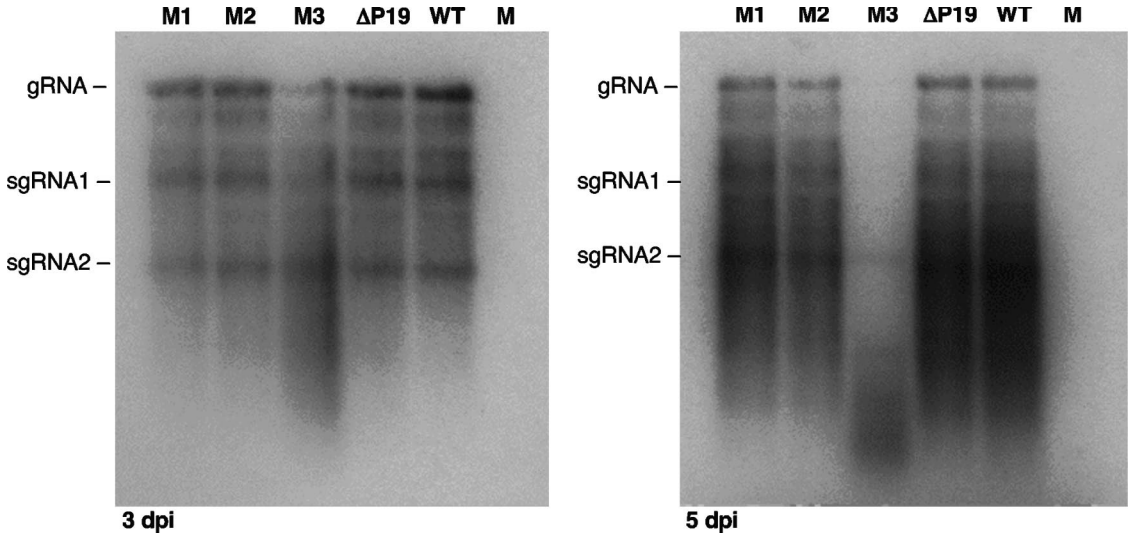

FIG. 8. Viral RNA maintenance in infected *N. benthamiana*. Total RNAs were extracted from infected *N. benthamiana* 3 dpi (left) and 5 dpi (right) with TBSV expressing M1, M2, M3, ΔP19, and wtP19 (WT). For Northern blot hybridization, dCTP-^{32}P-labeled full-length TBSV cDNA was used as a template for generating the probe.

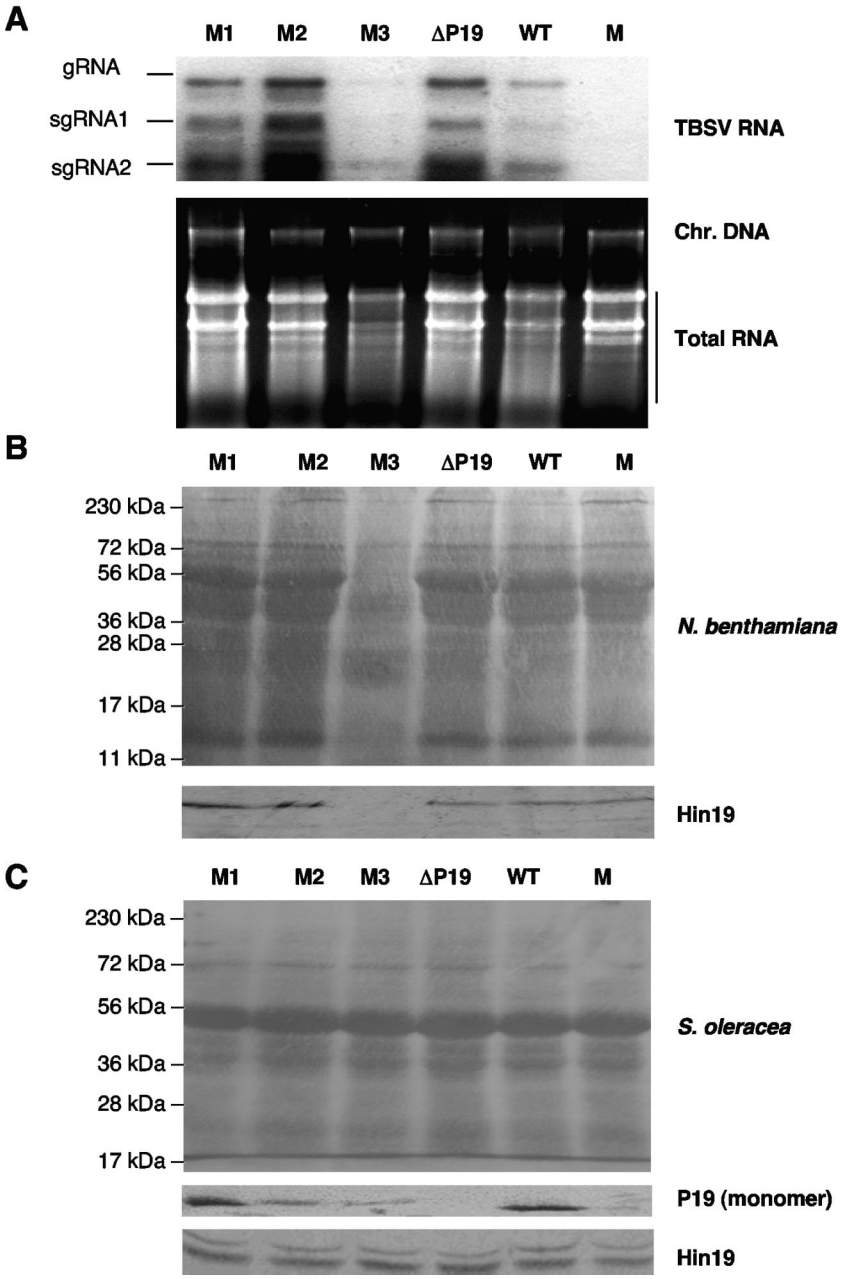

FIG. 9. Effect of M3 modifications on host RNA and protein in *N. benthamiana* versus spinach. (A) The top panel shows a Northern blot analysis for detection of TBSV RNAs in the total RNAs extracted at from *N. benthamiana* plants 7 dpi with selected P19 derivatives: M1, M2, M3, ΔP19, wtP19 (WT), and mock treatment (M). The lower panel shows the effect on host RNA integrity as evident for the reduced levels of rRNAs. (B) The upper panels show PonceauS staining of proteins from infected *N. benthamiana* plants. The bottom panel shows the accumulation of Hin19 as detected by a Western blot. (C) Total protein accumulation in extracts from infected spinach (top) and Western blots for P19 (middle) and Hin19 (bottom).

host RNAs, including rRNAs, were present in reduced amounts and/or degraded in extracts from plants infected with M3 (Fig. 9A, bottom) compared to the others.

Perhaps even more surprising than the effects associated with M3 on the accumulation of host RNA is what can be observed for the level of host proteins. When the total host protein amounts were compared (Fig. 9B, top), it was consistently observed that host proteins were substantially reduced in *N. benthamiana* plants infected with M3. This was not due to degradation during the extraction procedure because mixing of other samples with the M3 sample during extraction did not result in degradation of the exogenously supplied protein. Therefore, the reduction in levels of host material occurred in plants during infection with M3. Moreover, the levels of the P19-interactive host protein Hin19 were essentially undetectable in these samples (Fig. 9B, bottom). In contrast, this diminishing effect associated with M3 on virus and host material was not observed in duplicated experiments in pepper (data

not shown) and spinach (Fig. 9C). For instance, extracts from spinach leaves infected with M3 exhibited levels of total protein (top) and Hin19 (bottom) that did not dramatically deviate from what was observed for the other treatments (Fig. 9C). The levels of P19 are shown for comparison (Fig. 9C, middle panel) and display the same trend as shown in Fig. 6 for inoculated spinach leaves. Evidently, the M3 modifications substantially modulate host-dependent effects on the integrity of viral and host RNAs and proteins, and this property might very well be linked to the severe deformations observed upon the infection of systemically susceptible *Nicotiana* species.

DISCUSSION

Diverse symptoms are associated with siRNA binding mutants of P19 in *N. benthamiana*. Important properties of P19 that govern silencing suppression by siRNA appropriation include: (i) early and abundant accumulation of P19 upon infection; (ii) the capacity of P19 to use hydrogen bonds, salt bridges, and hydrophobic interactions to form a homodimer; (iii) the proper structural positioning of tryptophane residues on the P19 reading structure to precisely measure 21-nt siRNAs; and (iv) sequestration of siRNAs via ionic interactions with the sugar-phosphate backbone and 2′-hydroxyl groups of dsRNA (24, 27, 39, 51, 59).

In a previous biochemical study of P19 (24), it was shown that substitutions of residues at positions 75 and 78 caused a slight structural perturbation that, among other possible consequences, also prohibited the sequestration of siRNAs. This led to degradation of viral RNAs in infected *N. benthamiana* plants that subsequently recovered from infection several weeks after inoculation. The same study also showed that an Arg (R)-to-Trp (W) substitution at position 43 (P19/R43W) somewhat undermined the interaction with TBSV-derived siRNAs. Even though R43 was not predicted to represent an siRNA contact site, the mutation apparently compromised the functionality of nearby sites (W^{39}, T^{40}, and W^{42}) (Fig. 1) necessary for proper electrostatic interaction with siRNA (34). This unstable siRNA binding by P19/R43W was sufficient to lead to programming of an antiviral RISC that could be isolated and that was shown to specifically cleave TBSV RNA in vitro (25).

Despite the interesting properties associated with the aforementioned mutants (9, 24, 25, 49), nonspecific general effects due to structural perturbations on P19 could not be ruled out, and none of the studied mutants had been specifically designed to change siRNA binding sites. Therefore, one goal of the present study was to more precisely ascertain the role of the predicted siRNA binding sites for the various host-dependent biological roles of P19. Support for this type of approach came from studies showing that specific amino acid changes could substantially influence siRNA binding in vitro by the alkylation of cysteine residues (34). Therefore, the targeting of predicted siRNA binding sites would provide an opportunity to examine the biological significance of siRNA binding and at the same time permit an in vivo verification of the in vitro P19-siRNA structure prediction (51, 59).

In the present study 13 predicted siRNA binding residues on P19 were targeted for substitutions, either individually or as combinations (Table 1). The structural distributions of the selected P19 residues can be categorized into three major groups (Fig. 1): those affecting mostly peripheral residues on the P19 dimer (domain 1), those that involve the central domain of P19 (domain 3), and those that modified residues in the intermediate region between the peripheral reading head and the central part of the P19 dimer (domain 2). Irrespective of the substitutions, all of the mutants were infectious upon inoculation of *N. benthamiana*, and the progression of systemic infection at early stages was not impeded for any of the mutants. This agrees with previous observations that P19 is dispensable for initial infection of *N. benthamiana* (38) and that none of the mutations targeted essential *cis*-acting regions necessary for translation or replication (57). At the early stage of infection (3 dpi), P19 was not detectable for many mutants in *N. benthamiana*, but at 7 dpi P19 (and other virus proteins) readily accumulated, especially the SDS-recalcitrant dimer, for most P19 mutants (Table 1 and Fig. 3).

Mutations affecting domain 3 caused an exacerbation of symptoms compared to those associated with P19/K60A (domain 2), whereas those affecting domain 1 mostly resulted in attenuation of symptoms (Table 1 and Fig. 1). No consistent correlation was observed between the number of substitutions and effects on symptoms or between the relative level of P19 accumulation and the symptom severity (Table 1 and Fig. 3). The symptom attenuation and recovery phenotype previously observed for P19/R43W was predicted to affect the proper positioning of W^{39} and W^{42} in domain 1 and thus the strength of the P19-siRNA association (9, 24). This resembles the effect shown in the present study for the mutants in which precisely these residues (W^{39} and W^{42}) were substituted. Therefore, collectively the findings support the notion that W^{39} and W^{42} are involved in proper stacking of residues for efficient siRNA measuring and binding at the reading head.

The exacerbation of symptoms associated with some substitutions on P19 (compared to P19/K60A) suggest that certain host responses are induced, but the role of P19 in these particular instances might be diminished because its accumulation or stability was reduced. Perhaps parameters, in addition to P19 accumulation, contribute to symptom development in *N. benthamiana* that only surface in the context of certain P19 substitutions.

siRNA accumulation and sequestration. Three mutants (M1 to M3) were selected based on the symptoms, P19 accumulation, and position criteria detailed in Results, and these were subjected to further scrutiny; first, with regard to siRNA accumulation. The results showed that TBSV siRNAs were present in total RNAs of *N. benthamiana* plants infected with the wild type and mutants. These virus-associated siRNAs were double stranded and present in a distinct band of small RNAs that was specific for infected plants (Fig. 4) and simply detectable upon EtBr staining of agarose gels. This represents a very rapid and convenient indicator for TBSV infection and the appearance of TBSV-induced siRNA production at various stages during infection. This method, as well as the traditional Northern detection of siRNAs (Fig. 4), showed that the amount of total virus-derived siRNAs in *N. benthamiana* plants infected with the mutants was generally comparable to that observed for plants infected with virus expressing wtP19. This agrees with our previous studies for other P19 mutants (24, 25) and confirms that P19 has no effect on the accumulation of total TBSV

siRNAs with the realization that the total siRNAs obtained with the extraction procedure includes siRNAs sequestered by P19 inside infected cells. The exception with regard to total TBSV siRNA accumulation in the present study was M3, for which trace amounts of viral siRNAs could only be detected a few days after infection but, afterward, these were not detectable (Fig. 4, and data not shown).

Upon immunoprecipitation of P19 from infected plants, siRNAs were only detectable for wtP19 but not at detectable levels for the M1 to M3 mutants. These results provide confirmation that the residues on P19 predicted to bind siRNAs in vitro (51, 59) are also involved in binding virus-derived siRNAs during infection of plants. Substitutions of the siRNA binding sites in M1 and M2 prevented siRNA sequestration to cause the attenuation of symptoms culminating in the recovery of plants from infection. This suggests that failure of M1 and M2 to capture siRNAs resulted in activation of the RNAi machinery and programming of RISC. However, because P19 did not accumulate at readily detectable levels for M3 (and related combinatorial mutants with the S124P substitution) a correlation between symptom attenuation and siRNA sequestration could not be established.

From these results it is evident that some siRNA binding mutations compromise the RNA-protein interaction binding, as predicted based on the structure, to result in RNA silencing-mediated recovery (38, 51, 59). Detectable P19 accumulation and effective siRNA binding were thought to be required and sufficient for symptom attenuation (due to silencing), at least for wtP19 (38). However, this does not appear to be the case for some P19 mutants because specific siRNA binding site mutations (such as those in M3) provide unique and unexpected effects such as rapidly diminishing levels of viral RNA and siRNA accumulation (Fig. 4 and 8), symptom exacerbation (Table 1 and Fig. 2), and substantially reduced P19 accumulation (Fig. 3). Thus, the correlation between the inability of P19 mutants to sequester siRNAs and the attenuation of symptoms (indicative of RNAi-mediated recovery) is not strict in *N. benthamiana*.

Host-specific P19-mediated activities of siRNA-binding mutants. P19 is dispensable for TBSV replication in all hosts tested but, depending on the plant species, it is involved in different aspects of the infection process (38). For instance, P19 has a crucial role in systemic TBSV invasion of pepper and spinach (9, 49). The results of the present study showed that only wtP19 is active to allow TBSV infection of *N. gossei* and pepper, while all siRNA binding mutants were compromised for this pathogenicity. On the other hand, these same siRNA binding mutants were able to cause severe symptoms on spinach (Fig. 5), and TBSV RNA and protein accumulated (data not shown and Fig. 6). However, the P19-siRNA binding site mutants M1 to M3 were compromised for long-distance spread in spinach, as evidenced by a lack of P33 accumulation (Fig. 6). The observation that for mutants M1 and M3 P19 can be detected in upper leaves while P33 was undetectable agrees with observations that P19 is generally the first viral protein that accumulates at detectable levels through spinach (H. Scholthof, unpublished data).

At this point it is unknown what is responsible for the host-dependent activities or effects of wtP19 and/or its mutants. Even though we grew plants under comparable conditions, it is known that silencing-mediated events are temperature dependent (31, 46); thus, we cannot rule out that this affects the silencing and the siRNA sequestration differently dependent on the plant species. Nevertheless, altogether the results suggest that the integrity of siRNA binding sites on P19 and associated siRNA-binding are required in some hosts for infection, whereas in other species additional factors contribute to P19-mediated pathogenicity effects.

What are the factors other than siRNA binding that could contribute to these observations? It is known that a certain type of RNA export protein (ALY or Hin19) of *Arabidopsis* and *N. tabacum*, interacts with P19 even though the functional role, if any, of this interaction is not yet clear (6, 27, 50). However, it seems reasonable to consider that host factors might contribute to the function of P19, and our results suggest that these operate in an siRNA-binding independent manner. This assertion is supported by the finding that ALY proteins do not seem to be involved in silencing or P19-mediated suppression (6, 50). Furthermore, our previous studies showed that P19 functions as the elicitor of an HR in some hosts, and the onset of necrosis in the induced lesions is genetically not linked to the activation of a resistance response (9, 41). As an extension, the present study shows that in the absence of siRNA binding, a resistance response is still activated in *N. tabacum* (Fig. 5 and Table 2). Therefore, neither induction of necrosis nor siRNA binding are properties of P19 crucial for its ability to mount an effective HR. Although it cannot be ruled out that in local lesion hosts other than *N. tabacum*, P19-mediated activation of resistance may be linked to siRNA appropriation, the information to date suggests that P19 siRNA binding-independent properties contribute to the overall host-dependent functionality or effect of P19. This also agrees with the conclusion reached above regarding the aberrant behavior associated with M3.

Collectively, the results obtained with different plant species indicate the existence of a functional correlation between the ability of TBSV P19 to sequester siRNAs and the systemic invasion of spinach and pepper. Even though this supports the notion that suppression-mediated viral maintenance is a prerequisite for systemic invasion, the results with the pathogenic M3 that does not accumulate detectable levels of viral material provide an intriguing paradox.

Virus and host RNA and protein levels associated with mutants containing S124P. Why do mutants such as M3 with the S124P substitution cause severe leaf-deforming symptoms? It has been suggested that part of the symptomatology induced by P19 may be caused by its interaction with host-encoded miRNAs (7, 26), even though recent in vitro experiments suggest that P19 has a relatively weak affinity for miRNAs (8). Nevertheless, a potential and important miRNA binding property could be altered by the substitutions in M3. Unfortunately, the P19 protein accumulation for this mutant was reduced to such an extent that it was not possible to test whether it sequestered one or more specific miRNAs during the onset of infection.

Normally, the RNAi-mediated clearance of viral RNA in *N. benthamiana* plants infected with P19-defective mutants occurs not earlier than a week after infection (24). The results obtained with M3 provide a stark contrast with this "normal" course of events, because Northern blot analyses showed that

even though viral RNA accumulated to comparable levels for the mutants at 3 dpi, by 7 dpi the viral RNA had essentially disappeared from plants infected with M3 (Fig. 8 and 9). It is currently not known whether the vulnerability of the M3 RNA itself to RNAi is solely attributable to induction of activities by its encoded P19 or whether the nucleotide mutations have rendered this viral RNA especially susceptible to RNAi-mediated clearance compared to the other mutants. Furthermore, the mechanisms behind this RNA silencing acceleration may be related to preliminary findings that M3 siRNAs are detectable at 3 dpi but not until 5 dpi for wtTBSV.

In this context of accelerated RNA silencing combined with severe symptoms, it is also conspicuous that in *N. benthamiana* plants infected with M3, the levels of virus proteins (e.g., P19 in Fig. 3 and 9) and the P19-interactive Hin19 (Fig. 9) were strongly reduced. Even though accelerated viral RNA silencing could perhaps be predicted to cause concomitant loss of virus proteins, it was quite unexpected that the total host RNA and protein levels were also far less abundant in these inoculated *N. benthamiana* plants (Fig. 9). This dramatic change in physiological conditions was reflected in the preliminary observation that extracts from *N. benthamiana* plants infected with M3 rapidly colored brown during extraction in immunoprecipitation buffer (pH 7.5) and the pH value dropped to 6, while extracts from plants infected with wild-type and other selected TBSV derivatives remained green for a prolonged period with a pH value of approximately 7 (not shown).

It is possible that the M3-mutant P19 protein triggers a reaction that is protein or (mi)RNA mediated. For example, the cascade could start with the rapid breakdown of the M3/P19-Hin19 interaction, followed by total physiological meltdown that could be responsible for the strong deforming symptoms. Why the plant does not succumb to these events might be related to the rapid clearance of virus that perhaps reestablishes some sense of balance. It is also quite striking that the effect of the M3 mutation on the integrity of viral and host materials in *N. benthamiana* was not evident in pepper or in spinach. Even though the explanation for this phenomenon remains obscure, it is a new example of the host-dependent repertoire of effects associated with P19 (38).

In conclusion, the results of the present study show that (i) P19 is quite sensitive to mutagenesis of siRNA binding sites resulting in compromised siRNA binding by P19 and loss of lethal necrosis on *N. benthamiana*; (ii) in this host, siRNA-binding modifications on the central domain of P19 result in more severe symptoms compared to those affecting peripheral regions; (iii) simple agarose gel-mediated detection of small RNAs that contain TBSV-siRNAs is a rapid indicator of infection; (iv) the integrity of siRNA binding sites is essential for infection of some hosts, whereas in other plants this is less important and additional factors contribute; and (v) the M3 modifications on P19 lead to remarkable symptoms associated with acceleration of RNAi and reduced levels of viral and host RNA and proteins (notably P19 and Hin19) in a host-dependent manner.

ACKNOWLEDGMENTS

We are grateful to Karen-Beth G. Scholthof for helpful discussions and editing the manuscript. We thank Dong Qi and Jessica Ciomperlik for helpful comments. We thank Tony Cole for kindly providing us with *N. excelsior* seed.

This study was supported by Texas AgriLife Research (TEX08387), and different components were enabled through awards to H.B.S. from the National Institutes of Health (1RO3-AI067384-01) and the USDA/CSREES-NRI-CGP (2006-35319-17211) and by funds from Plant Bioscience, Ltd.

REFERENCES

1. **Anandalakshmi, R., G. J. Pruss, X. Ge, R. Marathe, A. C. Mallory, T. H. Smith, and V. B. Vance.** 1998. A viral suppressor of gene silencing in plants. Proc. Natl. Acad. Sci. USA **95:**13079–13084.
2. **Baulcombe, D.** 2004. RNA silencing in plants. Nature **431:**356–363.
3. **Bernstein, E., A. A. Caudy, S. M. Hammond, and G. J. Hannon.** 2001. Role for a bidentate ribonuclease in the initiation step of RNA interference. Nature **409:**363–366.
4. **Bisaro, D. M.** 2006. Silencing suppression by geminivirus proteins. Virology **344:**158–168.
5. **Brigneti, G., O. Voinnet, W.-X. Li, L.-H. Ji, S.-W. Ding, and D. C. Baulcombe.** 1998. Viral pathogenicity determinants are suppressors of transgene silencing in *Nicotiana benthamiana*. EMBO J. **17:**6739–6746.
6. **Canto, T., J. F. Uhrig, M. Swanson, K. M. Wright, and S. A. MacFarlane.** 2006. Translocation of *Tomato bushy stunt virus* p19 protein into the nucleus by ALY proteins compromises its silencing suppressor activity. J. Virol. **80:**9064–9072.
7. **Chapman, E. J., A. I. Prokhnevsky, K. Gopinath, V. V. Dolja, and J. C. Carrington.** 2004. Viral RNA silencing suppressors inhibit the microRNA pathway at an intermediate step. Genes Dev. **18:**1179–1186.
8. **Cheng, J., S. M. Sagan, Z. Jakubek, and J. P. Pezacki.** 2008. Studies of the interaction of the viral suppressor of RNA silencing protein p19 with small RNAs using fluorescence polarization. Biochem. **47:**8130–8138.
9. **Chu, M., B. Desvoyes, M. Turina, R. Noad, and H. B. Scholthof.** 2000. Genetic dissection of tomato bushy stunt virus p19-protein-mediated host-dependent symptom induction and systemic invasion. Virology **266:**79–87.
10. **Ding, S. W., and O. Voinnet.** 2007. Antiviral immunity directed by small RNAs. Cell **130:**413–426.
11. **Hamilton, A., O. Voinnet, L. Chappell, and D. Baulcombe.** 2002. Two classes of short interfering RNA in RNA silencing. EMBO J. **21:**4671–4679.
12. **Hamilton, A. J., and D. C. Baulcombe.** 1999. A species of small antisense RNA in posttranscriptional gene silencing in plants. Science **286:**950–952.
13. **Hearne, P. Q., D. A. Knorr, B. I. Hillman, and T. J. Morris.** 1990. The complete genome structure and synthesis of infectious RNA from clones of tomato bushy stunt virus. Virology **177:**141–151.
14. **Kasschau, K. D., and J. C. Carrington.** 1998. A counterdefensive strategy of plant viruses: suppression of posttranscriptional gene silencing. Cell **95:**461–470.
15. **Lakatos, L., G. Szittya, D. Silhavy, and J. Burgyan.** 2004. Molecular mechanism of RNA silencing suppression mediated by the p19 protein of tombusviruses. EMBO J. **23:**876–884.
16. **Li, F., and S. W. Ding.** 2006. Virus counterdefense: diverse strategies for evading the RNA-silencing immunity. Annu. Rev. Microbiol. **60:**503–531.
17. **Lindbo, J. A., F. Silva-Rosales, W. M. Proebsting, and W. G. Dougherty.** 1993. Induction of a highly specific antiviral state in transgenic plants: implications for regulation of gene expression and virus resistance. Plant Cell **5:**1749–1759.
18. **Lu, R., A. Folimonov, M. Shintaku, W. X. Li, B. W. Falk, W. O. Dawson, and S. W. Ding.** 2004. Three distinct suppressors of RNA silencing encoded by a 20-kb viral RNA genome. Proc. Natl. Acad. Sci. USA **101:**15742–15747.
19. **Martelli, G. P., D. Gallitelli, and M. Russo.** 1988. Tombusviruses, p. 13–72. *In* R. Koenig (ed.), The plant viruses, vol. 3. Plenum Publishing Corp., New York, NY.
20. **Molnar, A., T. Csorba, L. Lakatos, E. Varallyay, C. Lacomme, and J. Burgyan.** 2005. Plant virus-derived small interfering RNAs originate predominantly from highly structured single-stranded viral RNAs. J. Virol. **79:**7812–7818.
21. **Molnar, A., F. Schwach, D. J. Studholme, E. C. Thuenemann, and D. C. Baulcombe.** 2007. miRNAs control gene expression in the single-cell alga *Chlamydomonas reinhardtii*. Nature **447:**1126–1129.
22. **Okinaka, Y., K. Mise, T. Okuno, and I. Furusawa.** 2003. Characterization of a novel barley protein, HCP1, that interacts with the Brome mosaic virus coat protein. Mol. Plant-Microbe Interact. **16:**352–359.
23. **Olson, A. J., G. Bricogne, and S. C. Harrison.** 1983. Structure of *Tomato bushy stunt virus* IV: the virus particle at 2.9Å resolution. J. Mol. Biol. **171:**61–93.
24. **Omarov, R., K. Sparks, L. Smith, J. Zindovic, and H. B. Scholthof.** 2006. Biological relevance of a stable interaction between the tombusvirus-encoded P19 and siRNAs. J. Virol. **80:**3000–3008.
25. **Omarov, R. T., J. J. Ciomperlik, and H. B. Scholthof.** 2007. RNAi-associated ssRNA-specific ribonucleases in *Tombusvirus* P19 mutant-infected plants and evidence for a discrete siRNA-containing effector complex. Proc. Natl. Acad. Sci. USA **104:**1714–1719.

26. **Papp, I., M. F. Mette, W. Aufsatz, L. Daxinger, S. E. Schauer, A. Ray, J. vanderWinden, M. Matzke, and A. J. M. Matzke.** 2003. Evidence for nuclear processing of plant microRNA and short-interfering RNA precursors. Plant Physiol. **132:**1382–1390.
27. **Park, J.-W., S. Faure-Rabasse, M. A. Robinson, B. Desvoyes, and H. B. Scholthof.** 2004. The multifunctional plant viral suppressor of gene silencing P19 interacts with itself and an RNA binding host protein. Virology **323:**49–58.
28. **Qiu, W. P., J.-W. Park, and H. B. Scholthof.** 2002. Tombusvirus P19-mediated suppression of virus induced gene silencing is controlled by genetic and dosage features that influence pathogenicity. Mol. Plant-Microbe Interact. **15:**269–280.
29. **Qu, F., and T. J. Morris.** 2005. Suppressors of RNA silencing encoded by plant viruses and their role in virus infection. FEBS Lett. **579:**5958–5964.
30. **Qu, F., T. Ren, and T. J. Morris.** 2003. The coat protein of turnip crinkle virus suppresses posttranscriptional gene silencing at an early initiation step. J. Virol. **77:**511–522.
31. **Qu, F., X. Ye, G. Hou, S. Sato, T. E. Clemente, and T. J. Morris.** 2005. RDR6 has a broad-spectrum but temperature-dependent antiviral defense role in *Nicotiana benthamiana*. J. Virol. **79:**15209–15217.
32. **Roth, B. M., G. J. Pruss, and V. B. Vance.** 2004. Plant viral suppressors of RNA silencing. Virus Res. **102:**97–108.
33. **Russo, M., J. Burgyan, and G. P. Martelli.** 1994. Molecular biology of *Tombusviridae*. Adv. Virus Res. **44:**381–428.
34. **Sagan, S. M., R. Koukiekolo, E. Rodgers, N. K. Goto, and J. P. Pezacki.** 2007. Inhibition of siRNA binding to a p19 viral suppressor of RNA silencing by cysteine alkylation. Angew. Chem. Int. Edit. **46:**2005–2009.
35. **Sambrook, J., E. F. Fritsch, and T. Maniatis.** 1989. Molecular cloning: a laboratory manual, 2nd ed. Cold Spring Harbor Laboratory Press, Cold Spring Harbor, NY.
36. **Scholthof, H. B.** 2007. Heterologous expression of viral RNA interference suppressors: RISC management. Plant Physiol. **145:**1110–1117.
37. **Scholthof, H. B.** 2005. Plant virus transport: motions of functional equivalence. Trends Plant Sci. **10:**376–382.
38. **Scholthof, H. B.** 2006. The *Tombusvirus*-encoded P19: from irrelevance to elegance. Nat. Rev. Microbiol. **4:**405–411.
39. **Scholthof, H. B., B. Desvoyes, J. Kuecker, and E. Whitehead.** 1999. Biological activity of two tombusvirus proteins translated from nested genes is influenced by dosage control via context-dependent leaky scanning. Mol. Plant-Microbe Interact. **12:**670–679.
40. **Scholthof, H. B., T. J. Morris, and A. O. Jackson.** 1993. The capsid protein gene of tomato bushy stunt virus is dispensable for systemic movement and can be replaced for localized expression of foreign genes. Mol. Plant-Microbe Interact. **6:**309–322.
41. **Scholthof, H. B., K.-B. G. Scholthof, and A. O. Jackson.** 1995. Identification of tomato bushy stunt virus host-specific symptom determinants by expression of individual genes from a potato virus X vector. Plant Cell **7:**1157–1172.
42. **Scholthof, H. B., K.-B. G. Scholthof, M. Kikkert, and A. O. Jackson.** 1995. Tomato bushy stunt virus spread is regulated by two nested genes that function in cell-to-cell movement and host-dependent systemic invasion. Virology **213:**425–438.
43. **Scholthof, K.-B. G., H. B. Scholthof, and A. O. Jackson.** 1995. The tomato bushy stunt virus replicase proteins are coordinately expressed and membrane associated. Virology **208:**365–369.
44. **Silhavy, D., and J. Burgyan.** 2004. Effects and side-effects of viral RNA silencing suppressors on short RNAs. Trends Plant Sci. **9:**76–83.
45. **Silhavy, D., A. Molnar, A. Lucioli, G. Szittya, C. Hornyik, M. Tavazza, and J. Burgyan.** 2002. A viral protein suppresses RNA silencing and binds silencing-generated, 21- to 25-nucleotide double-stranded RNAs. EMBO J. **21:**3070–3080.
46. **Szittya, G., D. Silhavy, A. Molnar, Z. Havelda, A. Lovas, L. Lakatos, Z. Banfalvi, and J. Burgyan.** 2003. Low temperature inhibits RNA silencing-mediated defence by the control of siRNA generation. EMBO J. **22:**633–640.
47. **Takeda, A., K. Mise, and T. Okuno.** 2005. RNA silencing suppressors encoded by viruses of the family RNA silencing suppressors encoded by viruses of the family *Tombusviridae*. Plant Biotechnol. **22:**447–454.
48. **Thomas, C. L., V. Leh, C. Lederer, and A. J. Maule.** 2003. Turnip crinkle virus coat protein mediates suppression of RNA silencing in *Nicotiana benthamiana*. Virology **306:**33–41.
49. **Turina, M., R. Omarov, J. F. Murphy, C. Bazaldua-Hernandez, B. Desvoyes, and H. B. Scholthof.** 2003. A newly identified role for the *Tomato bushy stunt virus* P19 in short distance spread. Mol. Plant Pathol. **4:**67–72.
50. **Uhrig, J. F., T. Canto, D. Marshall, and S. A. MacFarlane.** 2004. Relocalization of nuclear ALY proteins to the cytoplasm by the tomato bushy stunt virus P19 pathogenicity protein. Plant Physiol. **135:**2411–2423.
51. **Vargason, J. M., G. Szittya, J. Burgyan, and T. M. Tanaka-Hall.** 2003. Size selective recognition of siRNA by an RNA silencing suppressor. Cell **115:**799–811.
52. **Voinnet, O.** 2005. Induction and suppression of RNA silencing: insights from viral infections. Nat. Rev. Genet. **6:**206–220.
53. **Voinnet, O.** 2008. Post-transcriptional RNA silencing in plant-microbe interactions: a touch of robustness and versatility. Curr. Opin. Plant Biol. **11:**464–470.
54. **Voinnet, O.** 2008. Use, tolerance and avoidance of amplified RNA silencing by plants. Trends Plant Sci. **13:**317–328.
55. **Voinnet, O., Y. M. Pinto, and D. C. Baulcombe.** 1999. Suppression of gene silencing: a general strategy used by diverse DNA and RNA viruses of plants. Proc. Natl. Acad. Sci. USA **96:**14147–14152.
56. **Voinnet, O., P. Vain, S. Angell, and D. C. Baulcombe.** 1998. Systemic spread of sequence-specific transgene RNA degradation in plants is initiated by localized introduction of ectopic promoterless DNA. Cell **95:**177–187.
57. **White, K. A., and P. D. Nagy.** 2004. Advances in the molecular biology of tombusviruses: gene expression, genome replication, and recombination. Prog. Nucleic Acids Res. Mol. Biol. **78:**187–226.
58. **Yamamura, Y., and H. B. Scholthof.** 2005. Pathogen profile—Tomato bushy stunt virus: a resilient model system for studying virus-plant interactions. Mol. Plant Pathol. **6:**491–502.
59. **Ye, K., L. Malinina, and D. Patel.** 2003. Recognition of small interfering RNA by a viral suppressor of RNA silencing. Nature **426:**874–878.
60. **Zamore, P. D.** 2002. Ancient pathways programmed by small RNAs. Science **296:**1265–1269.